Mechanical behaviour of corroded prestressing steel strand.

Chiho JEON [1], Jaebin LEE [1], Changsu SHIM [1]
[1] Chung-Ang University, Seoul, South Korea

Contact e-mail: chihobeer@cau.ac.kr

ABSTRACT: Since the prestressed concrete structure was introduced, many cases on deterioration of the prestressing steel due to corrosion have been reported. Once the corrosion of the tendons is observed in existing bridges, engineers need to decide actions such as replacement, strengthening and repair according to the conditions. In this paper, hundred corroded prestressing steel strands were obtained from the existing prestressed concrete bridges and inspected. For the engineering decision, the mechanical properties of tensile strength and fracture strain according to section loss by corrosion were evaluated by tensile tests. Three different configurations of section losses were defined to stand for the corrosion shape for quantitative evaluation, and empirical equations of remained tensile strength and fracture strain were proposed with respect to the section loss. Based on the observed behaviour of the corroded strands, equivalent analysis models of corroded strands were suggested for the evaluation of structural behaviour of prestressed concrete structures, and the model was verified by comparison to test results.

1 INTRODUCTION

In recent years, corrosion of prestressing steel has become a serious problem because it is hard to be detected and may lead to sudden collapse of prestressed concrete member. In addition, the corrosion in prestressing steel is not acceptable damage because it is not considered in design. However, it is impossible for budget reasons to replace all the tendons, therefore, understanding the mechanical behavior of corroded tendons become important so that maintenance official can judge the maintenance plan.

Since the first collapse of a segmental post-tensioned bridge due to corrosion of prestressing tendons, Bickton Meadows Bridge in the U.K in 1967 (Poston and Wouters 1998), was recorded, many inspection project have been performed in the U.K, Japan, Austria, United states, and so on. Reis (2007), Trejo (2009), and VDOT (2013) studied the corroded strands with visual inspection. They confirmed prestressing steel in an aged bridge had corrosion and found the reduction of strength through experimental research. However, they could not suggest the method to define the behavior quantitatively. Rinaldi et al. (2010), Xia et al. (2013), and Wu et al. (2016) adopted an electrochemical acceleration technique to generate the corrosion of the strands and conducted experiment. The researchers who used this technique, traditionally, considered mass loss as a corrosion parameter to define the mechanical behavior. This may not be compatible with the aged mechanical theory that the minimum cross-section governs the behavior of the tensile member, because measuring mass loss accumulates the damage of every cross-section along the length. Therefore, many researchers suggested the method to measure the reduced cross-section using pit depth and pit configuration to define the corrosion property of prestressing strands.

Stewart (2009) also proposed similar shape of pit configuration in rebar. Hartt and Lee (2016) proposed planar pit configuration. Lu et al. (2016) suggested hemispherical pit configuration based on Val and Melchers (1997) model. Lu et al. (2016) also suggested the damage constitutive model of corroded strand according to the damage factor using spring model. In this paper, three types of pit configuration adopted from previous research (Jeon et al. 2019) and reduction of mechanical properties are introduced from tensile test of corroded strands.

2 INSPECTION OF CORRODED STRANDS

In order to study on characteristic of corrosion in prestressing strands, 70 seven wire corroded strands (23 strands with diameter of 12.7 mm and 47 strands with diameter of 15.2 mm) taken from external tendon of an aged PSC box girder bridge were investigated. The length of each specimen was about 1,000 mm for tensile test, and pit depth of six outer wires in a cross section of the specimens was measured using pit depth gauge at 20 mm intervals; a total of 50 measurements were made at each specimen. This is to find the location of most corroded section and its section loss. Rust at surface of the specimens had removed using steel brush and rust remover before it is measured.

In the previous research (Jeon et al., 2019), the inspection resulted that a single-pit configuration cannot represent all the corrosion features. Therefore, three types of corrosion-induced pit configurations and formulas (Eq. 1~6) for calculation of its section loss were introduced. Fig. 1 shows the suggested pit configurations and corresponding corrosion features found in the inspection of corroded strands. The grey area in the figure is the residual cross-section. The formulas have been proposed to allow the investigator to measure the corrosion cross-section with little effort in the maintenance site (only measuring the pit depth of the corrosion wire).

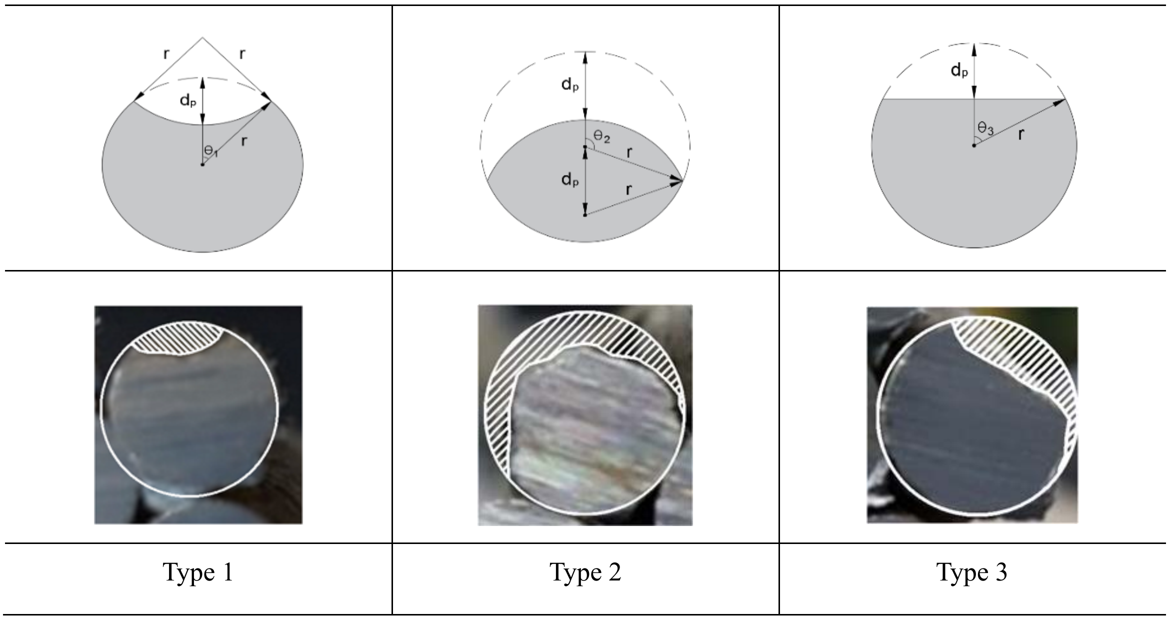

Figure 1. Pit configurations (Jeon et al. 2019)

The loss of sectional area can be calculated through the Eq. (1)-(6).

$$A_{sl,1} = 2r^2(\theta_1 - sin\theta_1 cos\theta_1) \quad for\ 0 \leq d_p \leq 2r \tag{1}$$

$$\theta_1 = \arccos\left(1 - \frac{d_p}{2r}\right) \tag{2}$$

$$A_{sl,2} = r^2(2\theta_2 - \pi - 2sin\theta_2 cos\theta_2) \quad for\ 0 \leq d_p \leq 2r \tag{3}$$

$$\theta_2 = \arccos\left(-\frac{d_p}{2r}\right) \tag{4}$$

$$A_{sl,3} = r^2(\theta_3 - sin\theta_3 cos\theta_3) \quad for\ 0 \leq d_p \leq 2r \tag{5}$$

$$\theta_3 = \arccos\left(1 - \frac{d_p}{r}\right) \tag{6}$$

Where, $A_{sl,1\text{-}3}$ are the loss of sectional area according to the type of pit configuration, r is the radius of a wire, and d_p is the pit depth measured by depth gauge at the deepest location.

3 MECHANICAL PROPERTIES OF CORRODED STRANDS

3.1 Mechanical properties of a corroded wire from FEM analysis

Seven wire steel strand investigated is composed of one core wire and six outer wires. The behaviour of the strands could be considered as a combination of the behavior of the wires. The mechanical properties of the wire were derived from the Finite Element Method (FEM) analysis modelled with the parameters of pit depth, width, and configurations as shown in Fig. 2(Jeon et al., 2009). The yield stress and strain according to the type of section loss, and the ultimate stress and strain are expressed with Eq. (7) ~ (10) and summarized in Table 1. The material model of the wire is defined as bi-linear model with properties from tensile test in Fig. 5

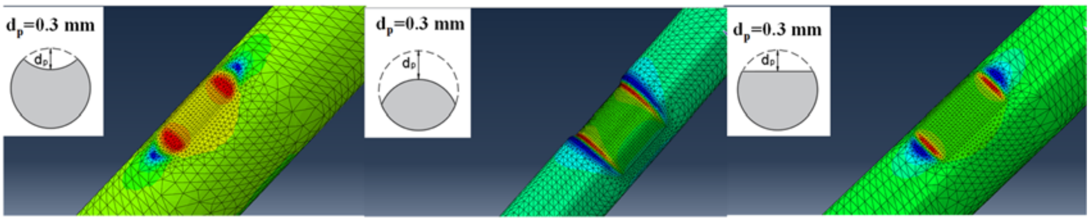

Figure 2. FEM models of the corroded wire

$$f_{y.c} = 0.85 f_{u.c} \tag{7}$$

$$\varepsilon_{y.c} = \frac{0.85 f_{u.c}}{E_s} \tag{8}$$

$$f_{u.c} = a\eta + b \tag{9}$$

$$\varepsilon_{u.c} = \begin{cases} c\eta^2 + d\eta + e & for \quad d_p < 0.5 \\ f\eta^g & for \quad d_p \geq 0.5 \end{cases} \tag{10}$$

Where, $f_{y.c}$ and $\varepsilon_{y.c}$ are the yield stress and strain of corroded wire, respectively. $f_{u.c}$ and $\varepsilon_{u.c}$ are the ultimate stress and strain of corroded strand, respectively. η is section loss calculated by loss of cross-sectional area (A_{sl})/original cross sectional area (A_0). The coefficients a, b, c, d, e, f, and g are parameters to define the ultimate mechanical properties of a corroded wire from the previous study (Jeon et al., 2019).

Table 1. Coefficients for Eq. (9) and (10)

Pit configuration	**Coefficients**						
	a	b	c	d	e	f	g
Type 1	-1991.8	1748.0	-5.96	-1.30	0.0754	0.0025	-0.621
Type 2	-1995.6	1801.6	-1.00	-0.69	0.0754	0.0045	-0.305
Type 3	-2302.7	1752.7	9.54	-1.77	0.0754	0.0045	-0.298

Using Eq. (7), (8), (9), and (10), stress-strain relation of a corroded wire can be mathematically expressed as follow:

$$\sigma_w(\varepsilon) = \begin{cases} E_s \cdot \varepsilon & \varepsilon < \varepsilon_{y.c} \\ 0.85 f_{u.c} + \frac{\varepsilon - \varepsilon_{y.c}}{\varepsilon_{u.c} - \varepsilon_{y.c}} \cdot 0.15 f_{u.c} & \varepsilon_{y.c} < \varepsilon \le \varepsilon_{u.c} \end{cases} \quad (11)$$

where, $\sigma_w(\varepsilon)$ is the stress of a wire with respect to ε.

3.2 Equivalent material model of a corroded strand using spring model

The behaviour of the strands could be considered as a combination of the behavior of the wires. Lu et al. (2016) suggested the damage constitutive model of corroded strand using spring model, and the spring model concept was adopted to express the behavior of corroded strand in the previous research (Jeon et al., 2019). Fig. 3 depicts an example of the spring model; four non-corroded wires and three corroded wires with different level of corrosion. Each spring means the stress-strain behavior of the wires defined by Eq. (11) based on section loss. Eq. (12) is mathematical expression of the spring model to predict the behavior of corroded strand.

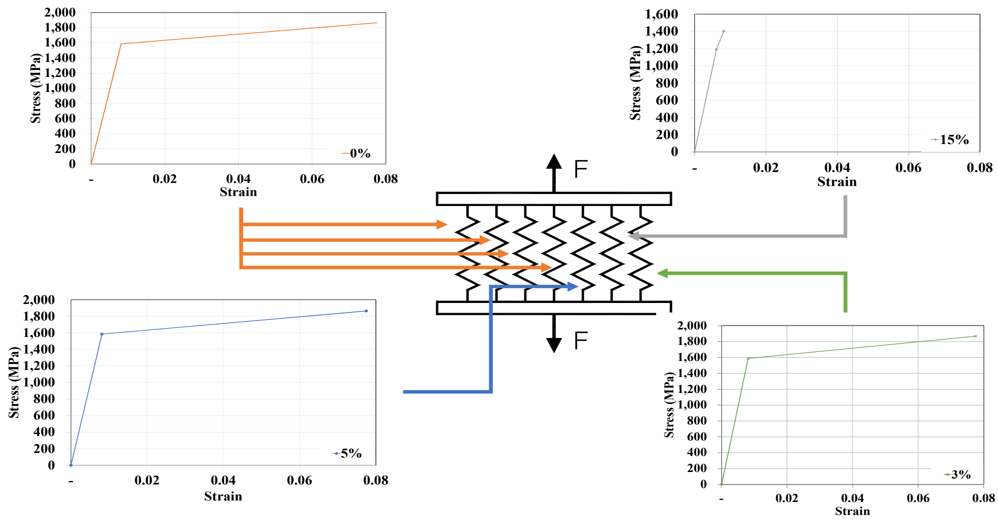

Figure 3. Spring model of a corroded strand composed of s-s relation of wires (Jeon et al. 2019)

$$\sigma_s(\varepsilon) = \frac{\sum_{i=1}^{n}(\sigma_{w,i}(\varepsilon)\cdot A_{0,i})}{\sum_{i=1}^{n}(A_{0,i})} \quad (12)$$

where, σ_s (ε) is the stress of a strand with respect to ε. $\sigma_{w,i}$ (ε) is the stress of a ith wire making up the strand, and $A_{0,i}$ is the cross sectional area of the *i*th wire.

4 TENSILE TEST OF CORRODED STRANDS

4.1.1 Test setup

The tensile tests were conducted with a universal testing machine as shown in Fig. 4. The specimens were loaded up to their failure by displacement control method with speed of 5 mm/min. The failure of corrosion was defined when any wire was fractured. In the tensile test, two end sides of the strand are held by the grip. If the grip wedge contacts the surface of a strand directly, crack can be propagated from the wedge earlier than the tensile strength of the wire due to stress concentration. For this reason, Kim et al. (2014) suggested to wrap the end parts with two silica-coated aluminum plates to protect the end parts. This method was adopted in this paper. The elongation was measured by displacement from the machine.

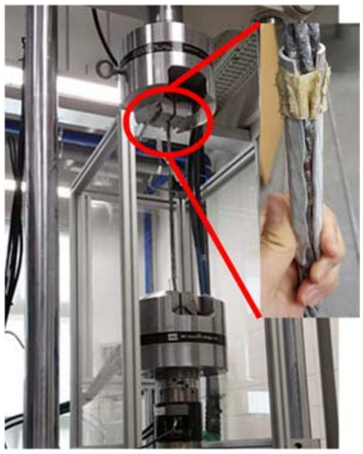

Figure 4. Test setup

Fig. 5 shows the result of tensile test of three non-corroded strands taken from aged bridge. The average elastic modulus of the strands is 195,000 MPa. The average yield strength and yield strain are 1628 MPa and 0.0083, respectively. The average ultimate strength and ultimate strain are 1,865 MPa and 0.075, respectively.

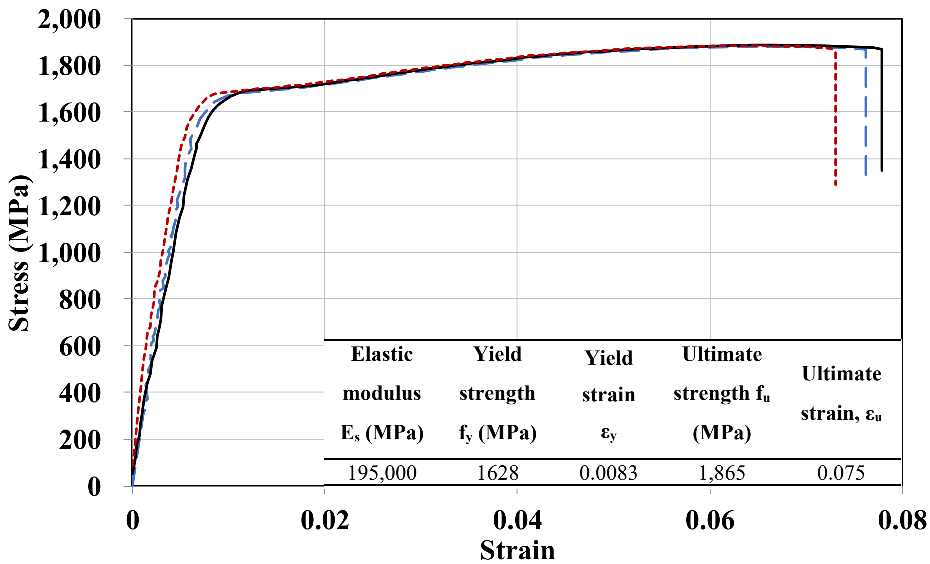

Figure 5. Stress-strain relation of non-corroded strands

4.1.2 Test result of corroded strands and comparison to the equivalent material model.

Fig. 6 shows the test result and its expected mechanical properties from equivalent material model of 70 corroded wires. The parameter to define the reduction of mechanical properties is section loss of the most corroded wire, because it is considered that the most corroded wire governs the behavior of a strand. The strength of the corroded strands was defined with ultimate normalized load due to two reasons. One is uncertain initial cross-section that makes engineering stress unmeasurable. Another is that two different types of strands (diameter of 12.7 mm and 15.2 mm) were tested. Regression lines are also depicted in the graphs, and the correlation between ultimate strain and section loss from suggested model is explained with two regression lines because the tendency of the correlation is changed based on 5% of section loss

The experimental results show relatively large variance due to irregular shape and distribution of corroded pits. It is considered that this reflects the material variability of the strand, the effect of frictional force between wires, and the difference between the actual section loss and the calculated section loss. In addition, the equivalent material model shows conservative prediction of an average of 0.11 in normalized ultimate strength and 0.015 in ultimate strain. Regression lines of the results also show steep reductions in strength and ultimate strain with increasing section loss. This means the equivalent material model gives the minimum reduced mechanical properties of corroded strands, which is adoptable to decision making on maintenance of aged PSC structures.

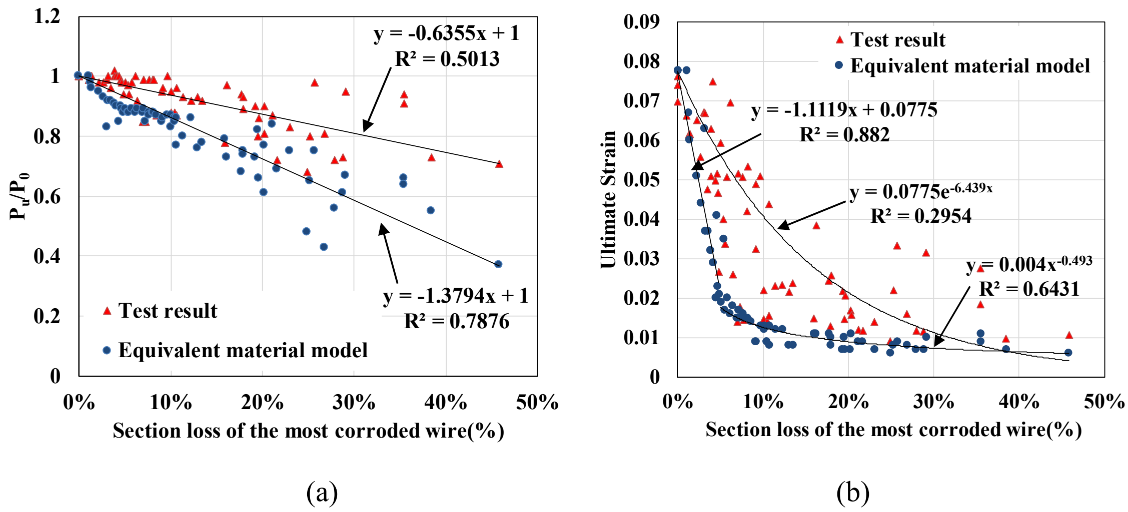

Figure 6. Comparison between test result and the equivalent material model on (a) normalized ultimate strength and (b) ultimate strain.

5 CONCLUSION

In this paper, mechanical behaviour of corroded strands was introduced using equivalent material model. The model was verified by comparison to the tensile test result. The following conclusions were derived from the study

1) Three types of pit configurations and corresponding formulas were introduced to calculate the section loss of corroded prestressing strand wires.
2) The stress-strain relations of corroded wires were derived from FEM analysis, and the spring model was adopted to define the behavior of corroded seven-wire strand.
3) Tensile test of 70 corroded strands from an existing bridge were conducted and compared to the suggested equivalent material model. It was found that the equivalent

material model showed conservative prediction of an average of 0.11 in normalized ultimate strength and 0.015 in ultimate strain comparing to the test result.

ACKNOWLEDGEMENTS

This study was supported by a grant (19SCIP-B128570-03) from the Smart Civil Infrastructure Research Program funded by the Ministry of Land, Infrastructure and Transport (MOLIT) of the Korean government and the Korea Agency for Infrastructure Technology Advancement (KAIA).

REFERNCES

D Trejo, MBD Hueste, P Gardoni, RG Pillai, K Reinschmidt, SB Im, S Kataria, S Hurlebaus, M Gamble, TT Ngo, 2009, Effect of Voids in Grouted Post-Tesioned Concrete Bridge Construction: Electrochemical testing and Reliability Assessment. Austin: *Texas Transportation Institute*.

Hartt WH, Lee SK., 2016, Projecting Corrosion-Induced Bridge Tendon Failure Resulting from Deficient Grout: Part I–Model Development and Example Results. *CORROSION*, 72(8): 991-998.

Chiho Jeon, Jaebin Lee, Sokanya Lon, Chang-su Shim, (2019), Equivalent material model of corroded prestressing steel strand, Journal of Materials Research and Technology, (Summited)

Kim JK, Kim JS, Kwon SH., 2014, Mechanical Properties of a New Prestressing Strand with Ultimate Strength of 2160 MPa. *KSCE Journal of Civil Engineering*, 8(2): 607-615.

Lu ZH, Li F, Zhao YG., 2016, An Investigation of Degradation of Mechanical Behaviour of Prestressing Strands Subjected to Chloride Attacking. *Proceedings of International Conference on Durability of Concrete Structures*, Jun 30-Jul 1, Shenzhen University, Shenzhen, Guangdong Province: P.R.China.

Poston, R. W., and Wouters, J. P., 1998, Durability of Precast Segmental Bridges: Final Report. NCHRP Web Document No. 15, Project 20-7, Task 92, *National Cooperative Highway Research Program (NCHRP)*, Washington, DC..

Reis R A., 2007, Corrosion Evaluation and Tensile Results of Selected Post-Tensioning Strands at the SFOBB Skyway Seismic Replacement Project. *California Department of Transportation*, Sacramento.

Rinaldi Z, Imperatore S, Valente C., 2010, Experimental evaluation of the flexural behavior of corroded P/C beams. *Construction and Building Materials*, 24, 2267-2278

Stewart MG., 2009, Mechanical behaviour of pitting corrosion of flexural and shear reinforcement and its effect on structural reliability of corroding RC beams, Structural Safety. 31, 19-30.

Val DV, Melchers RE., 1997 Reliability of Deteriorating RC Slab Bridges. *Journal of Structural Engineering*. ASCE.,123(12): 1638-1644

VDOT. EVALUATION OF GROUT AND STRANDS AT 13 TENDON LOCATIONS AND SELECTED VERTICAL PT BARS AT FIXED PIERS: Maintenance and Repair using Corrosion Mitigation Systems (Final Report). *Virginia Department of Transportation*

Wu X, Li H., 2016, Effect of Strain Level on Corrosion of Prestressing Steel Strands. *Proceedings of International Association for Bridge and Structural Engineering*, Zurich, 292-299

Xia J, Jin WL, Zhao YX, Li LY., 2013, Mechanical performance of corroded steel bars in concrete. *Structures & Buildings*, 166(5): 235-246